

The Electric Dipole Moment Challenge, Including Stern-Gerlach Polarimetry

Richard Talman

Cornell, Laboratory for Elementary-Particle Physics

SLAC Seminar
21 July, 2016

2 Outline

Force Field Symmetries

Why Measure EDM?

BNL “AGS Analogue” Ring as EDM Prototype

Conceptual EDM Measurement Ring

Why “Rolling Polarization”? and Why the EDM Signal Survives

Octupole Only EDM Storage Ring “Self-Magnetometer Bottle”

Stern-Gerlach Polarimetry

Frequency Domain Treatment of Helical Resonator Response

Achievable Precision

Conclusions

Much of this talk is extracted from the following papers:

- ▶ R. and J. Talman, *Symplectic orbit and spin tracking code for all-electric storage rings*, Phys. Rev. ST Accel Beams **18**, ZD10091, 2015
- ▶ R. and J. Talman, *Electric dipole moment planning with a resurrected BNL Alternating Gradient Synchrotron electron analog ring*, Phys. Rev. ST Accel Beams **18**, ZD10092, 2015
- ▶ R. Talman, *Frequency domain storage ring method for Electric Dipole Moment measurement*, arXiv:1508.04366 [physics.acc-ph], 18 Aug 2015
- ▶ R. Talman, *Octupole focusing relativistic self-magnetometer electric storage ring “bottle”*, arXiv:1512.00884 [physics.acc-ph], 2 Dec 2015

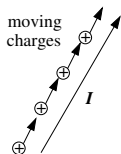
4 Force Field Symmetries: Vectors and Pseudovectors



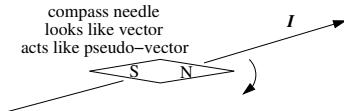
EDM =
charge \times separation
a vector



MDM =
current \times area
a pseudo-vector



current, I
a vector

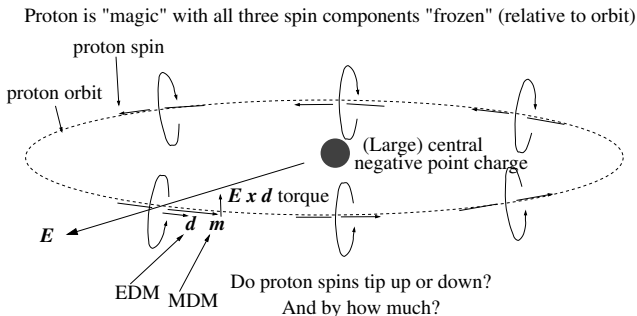


- ▶ An electric dipole moment (EDM) points from plus charge toward minus charge—the “orientation” of a true **vector**.
- ▶ The axis of a magnetic dipole moment (MDM) is perpendicular to a current loop, whose direction gives a different “orientation”. The MDM is a **pseudo-vector**.
- ▶ Ampère: how does the compass needle know which way to turn?

5 Capsule history of force field symmetries

- ▶ Newton: Gravitational field, (inverse square law) central force
- ▶ Coulomb: By analogy, electric force is the same (i.e. central)
- ▶ Ampere: How can compass needle near a current figure out which way to turn? Magnetic field is **pseudo-vector**. A **right hand rule** is somehow built into E&M and into the compass needle.
- ▶ The upshot: By introducing **pseudo-vector** magnetic field, E&M respects reflection symmetry, but compound objects need not exhibit the symmetry.
- ▶ Lee, Yang, etc: A particle with spin (**pseudo-vector**), say “up”, can decay more up than down (**vector**);
 - ▶ i.e. the decay vector is parallel (not anti-parallel) to the spin pseudo-vector,
 - ▶ viewed in a mirror, this statement is reversed.
 - ▶ i.e. weak decay force violates reflection symmetry (P).
- ▶ Fitch, Cronin, etc: protons, etc. have both MDM and EDM. This violates both parity (P) and time reversal (T).
- ▶ Current task: How to exploit the implied symmetry violation to measure the EDM of proton, electron, etc?

6 EDM Sensitive Configuration



Two issues:

- ▶ Can the tipping angle be measurably large for plausibly large EDM, such as 10^{-30} e-cm? With modern, frequency domain, technology, yes
- ▶ Can the symmetry be adequately preserved when the idealized configuration above is approximated in the laboratory? This is the main issue

7 Why Measure EDM?

- ▶ Violations of parity (P) and time reversal (T) in the standard model are insufficient to account for excess of particles over anti-particles in the present day universe.
- ▶ Any non-zero EDM of electron or proton would represent a violation of both P and T, and therefore also CP.

Comments:

- ▶ Beam direction reversal is possible (only) in all-electric storage ring, with all parameters except injection direction held fixed. This is important for reducing systematic errors.
- ▶ “Frozen spin” operation in all-electric storage ring is only possible with electrons or protons—by chance their anomalous magnetic moment values are appropriate. The “magic” kinetic energies are 14.5 MeV for e, 235 MeV for p.

8 BNL “AGS Analogue” Ring as EDM Prototype

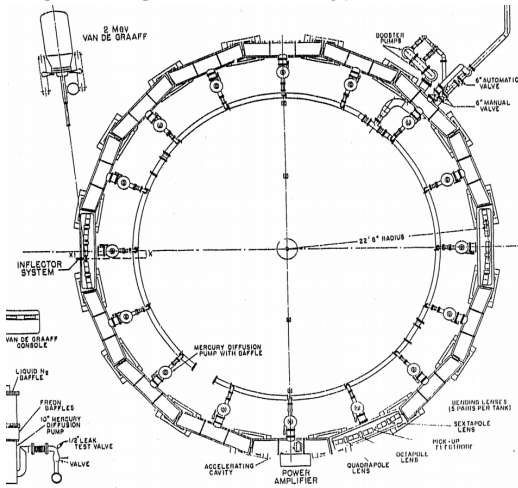


Figure: The 1955 AGS-Analogue lattice has been reverse engineered from available documentation—mainly the 1953 BNL-AEC proposal letter. Except for insufficient straight section length, and the 10 MeV rather than 14.5 MeV energy, this ring could be used to measure the electron EDM.

Field strength (magnetic type)	
at injection	10.5 gauss
at 10 MeV	74 gauss
Field strength (electrostatic type)	
at injection	3 kV/cm
at 10 MeV	22 kV/cm
Rise time	.01 sec
Phase transition energy	2.8 MeV
Frequency (final)	7 mc
Frequency change	5% %
Volts/turn	150 V
RF power	about 1 kw
No. of betatron wavelengths	about 6.2
aperture	1 X 1 in.
Betatron amplitude for 10^{-3} rad. error	0.07 in.
Maximum stable amplitude, synchrotron osc.	-0.16 in.
Radial spacing of betatron resonances	about 0.4 in.
Vacuum requirement	about 10^{-6} mm Hg

Total power requirements will be small and available with existing installations. The test shack seems to be a suitable location since the ring will be erected inside a thin magnetic shield which can be thermally insulated and heated economically.

We estimate the cost to be approximately \$600,000, distributed as shown in the following table:

<u>Model</u>	<u>Direct</u>	<u>Overhead</u>	<u>Total</u>	<u>Inflate to 2015</u>
Staff S. & W.	\$135,000	\$ 65,000	\$200,000	\$M 1.76
Van de Graaff	70,000	-	70,000	0.62
Other E. & S.	130,000	-	130,000	1.14
Shops	<u>135,000</u>	<u>65,000</u>	<u>200,000</u>	<u>1.76</u>
	\$470,000	\$130,000	\$600,000	\$M 5.27

10 EDM Measurement Ring

(passive) resonant polarimeters

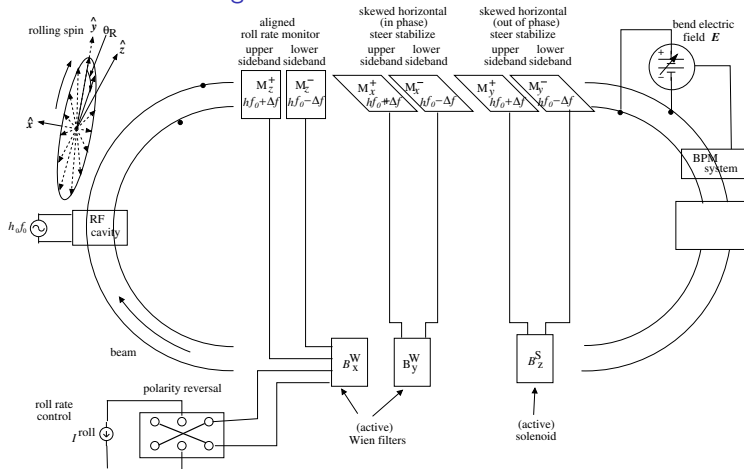


Figure: Cartoon of the EDM ring and its spin control. The Koop polarization “spin wheel” in the upper left corner “rolls” along the ring, always upright, and aligned with the orbit. The boxes at the bottom apply torques to the magnetic moments without altering the design orbit.

- ▶ Because of the rolling polarization the resonator excitation appears as upper and lower sidebands of the revolution frequency (and its harmonics).
- ▶ Elements with superscript “W” are Wien filters; superscript “S” indicates solenoid.
- ▶ **The frequency domain EDM signal is the difference between forward and backward spin wheel rotation frequencies, when the B_x^W Wien filter polarity is reversed.**
- ▶ EDM measurement accuracy (as contrasted with precision) is limited by the reversal accuracy occurring in the shaded region.
- ▶ Precision is governed by scaler precision. This is a benefit obtained by moving the EDM sensitivity from polarimeter intensity to polarimeter frequency response.

12 Why “Rolling Polarization”? and Why the EDM Signal Survives

- ▶ Polarized “spin wheel” was proposed by Koop to cancel $\Delta\gamma$ spin decoherence.
- ▶ Also the rolling polarization shifts the resonator response frequency *away from* harmonic of revolution frequency—away from direct charge response
- ▶ Since the roll torque is always parallel to the wheel axis it shifts the roll rate proportional to the EDM
- ▶ Reversing the roll direction (with beam direction fixed) does not change the EDM contribution to the roll.
- ▶ **The difference between forward and backward roll-rates measures the EDM (as a frequency difference).**

13 Storage Ring Rolling Magnetization Frequency Spectra

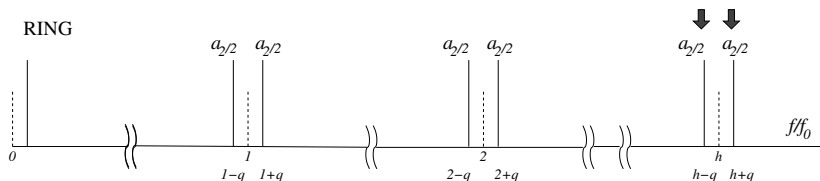


Figure: Frequency spectra of the beam polarization drive signal to the resonant polarimeter. Sideband spacings are vastly exaggerated. They are equal to the Koop roll frequency of order 1 KHz. The operative polarimetry sideband lines are indicated by dark arrows.

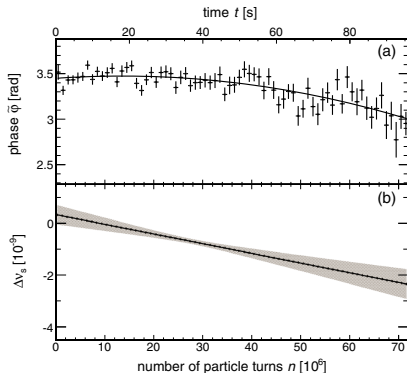


FIG. 3 (color online). (a) Phase $\tilde{\varphi}$ as a function of turn number n for all 72 turn intervals of a single measurement cycle for $|\nu_s^{\text{fix}}| = 0.160\,975\,407$, together with a parabolic fit. (b) Deviation $\Delta\nu_s$ of the spin tune from ν_s^{fix} as a function of turn number in the cycle. At $t \approx 38$ s, the interpolated spin tune amounts to $|\nu_s| = (16\,097\,540\,628.3 \pm 9.7) \times 10^{-11}$. The error band shows the statistical error obtained from the parabolic fit, shown in panel (a).

15 Octupole Only EDM Storage Ring “Self-Magnetometer Bottle”

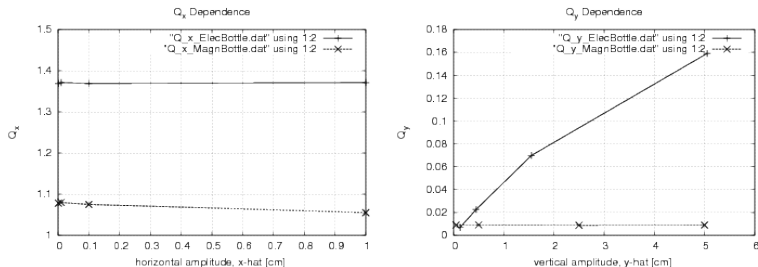


Figure: Horizontal and vertical tunes in octupole only electric and (conventional) quadrupole focusing magnetic relativistic storage ring bottles. The strikingly novel feature is the nearly proportional dependence of Q_y on vertical amplitude in the octupole-only electric case—this causes small vertical amplitude orbits are hypersensitive to radial magnetic field errors. This suppresses the leading source of systematic error.

16 Self-Magnetometer Bottle Sensitivity to Radial Magnetic Field

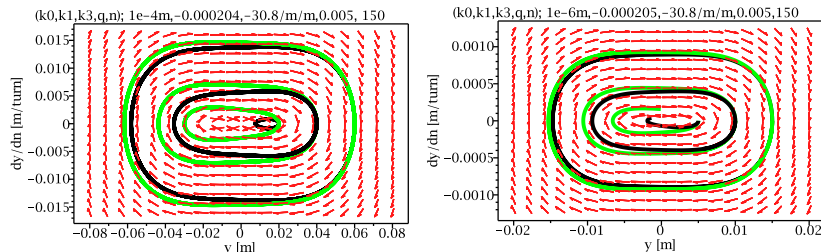


Figure: An radial magnetic field error is added intentionally. Small betatron amplitude on the left, large amplitude on the right, phase space orbits in relativistic self-magnetometer octupole-only electric storage ring “bottle” focusing. Green orbits are CW, black CCW.

17 Resonant Polarimeter (Transverse)

ON-AXIS BEAM THROUGH TE101 STERN-GERLACH POLARIMETER CAVITY

(candidate to canted TE101)

No aperture parameters

conductivity = $6.17\text{E}7$ Siem./m

f = 0.7507 GHz

Q = 30194

BW = 24.86 KHz

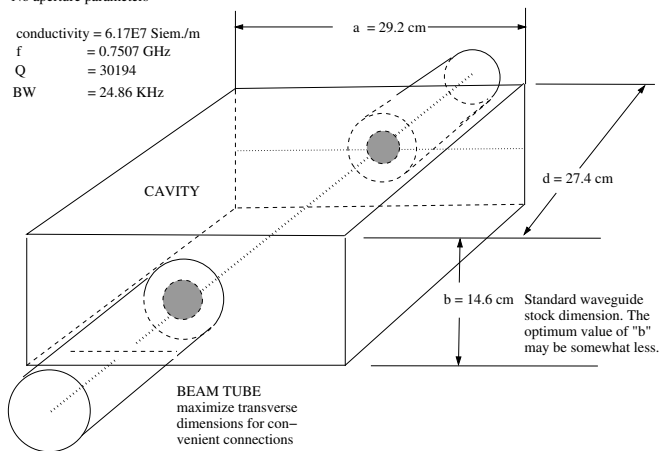


Figure: Candidate RF cavities for Stern-Gerlach (transverse) polarimetry. The cavity dimensions have been adjusted for a planned test at Jefferson Lab in a CEBAF extraction line.

18 Toggling-Polarization Beam for CEBAF Test

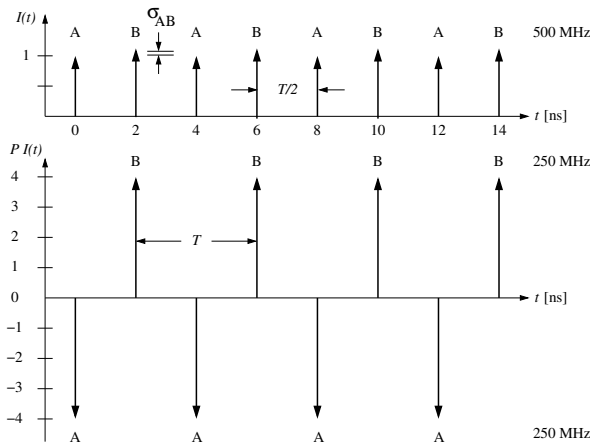


Figure: Beam A, 250 MHz, positive polarization bunches, alternate with beam B, 250 MHz, negative polarization bunches. (Except for σ_{AB} amplitude imbalance) the beam charge frequencies are harmonics of 0.5 GHz. i.e. 0.5, 1.0, 1.5, The beam magnetization frequencies are harmonics of 0.75 GHz. i.e. 0.75, 1.5, 2.25,

19 CEBAF Test Beam Frequency Spectra

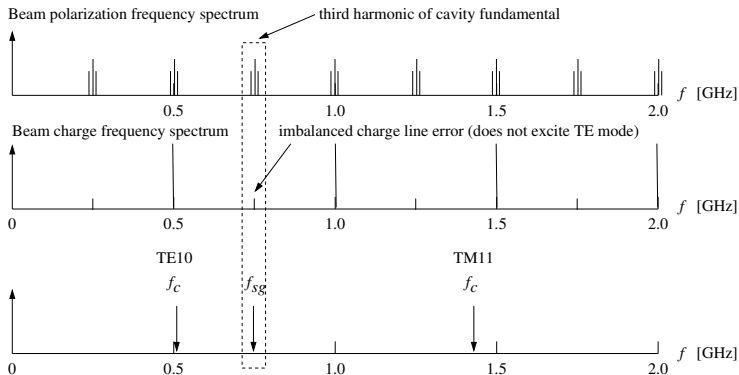


Figure: The top plot shows frequency spectra of each (staggered) A and B bunch currents. There is the possibility of beam magnetization side bands if the A and/or B polarization frequencies are being modulated and $P_A I_A$ or $P_B I_B$ is plotted. The middle plot shows the frequency spectrum of the total bunch current. The dominant lines are at twice the frequency of the individual currents. Mismatch of A and B currents produces background lines coinciding with magnetization lines. The bottom plot indicates the f_{S-G} frequency to which the resonator is tuned, the cut-off frequency of the fundamental, S-G sensitive TE₁₀ mode, and the lowest frequency charge-sensitive TM₁₁ mode.

20 Resonant Polarimeter (Longitudinal)

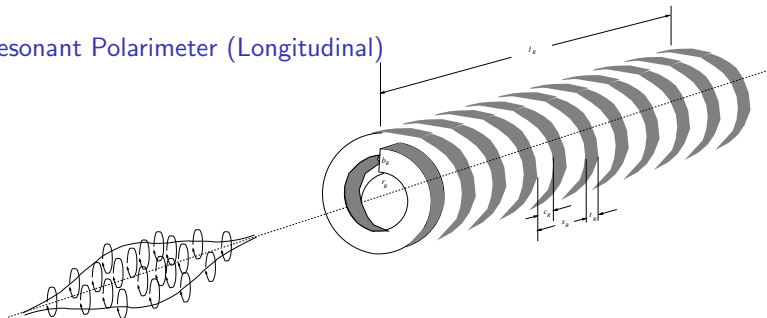


Figure: Longitudinally polarized beam approaching a superconducting helical resonator. Beam polarization is due to the more or less parallel alignment of the individual particle spins, indicated here as tiny current loops. The helix is the inner conductor of a helical transmission line, open at both ends. The cylindrical outer conductor is not shown.

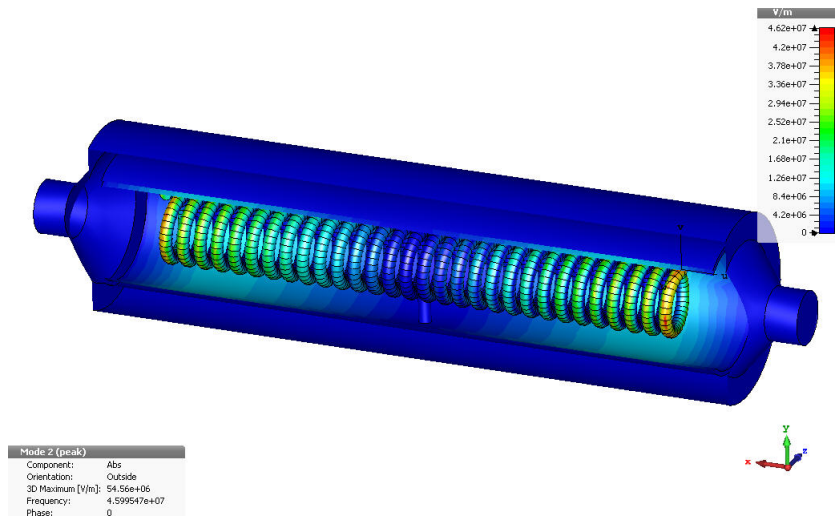


Figure: Evgeny Zaplatin (Jülich) CAD drawing for resonant polarimeter roughly matched for particle speed $\beta_p \approx 0.2$, wave speed $\beta_r \approx 0.1$.

22 Helical polarimeter room temperature bench test

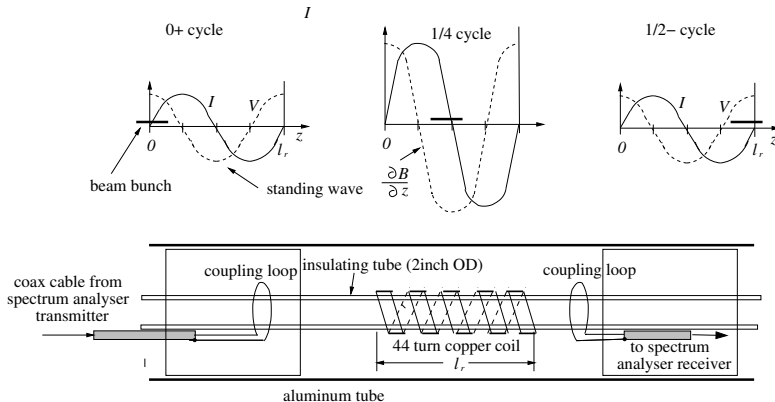


Figure: . Room temperature bench test set-up of prototype resonant polarimeter, with results shown in next figure. The coil length is $l_r=11$ inches. Beam magnetization is emulated by the spectrum analyser transmitter.

- ▶ Resonator excitation is detected by a single turn loop connected to the spectrum analyser receiver.
- ▶ This would be an appropriate pick-up in the true polarimetry application though, like the resonator, the preamplifier would have to be at cryogenic temperature to maximize the signal to noise ratio.
- ▶ The figures above the apparatus are intended to complete the analogy to a situation in which the transmitter is replaced by the passage of a beam bunch.
- ▶ The particle and wave speeds are arranged to maximize the energy transfer from beam to resonator.

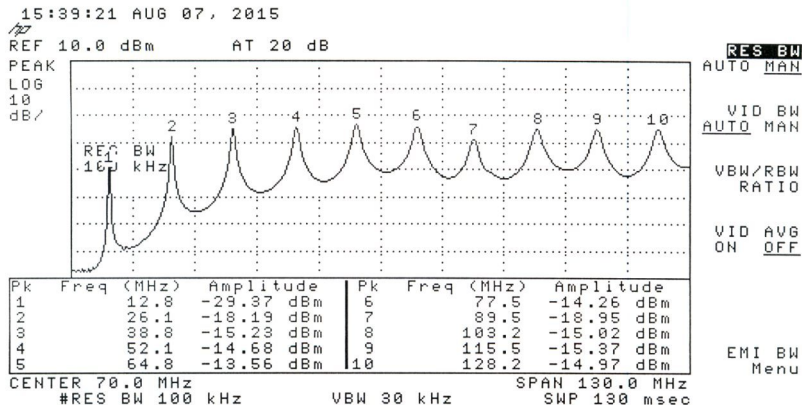


Figure: Frequency spectrum observed using the bench test shown in previous figure. Ten normal modes of the helical transmission line are visible.

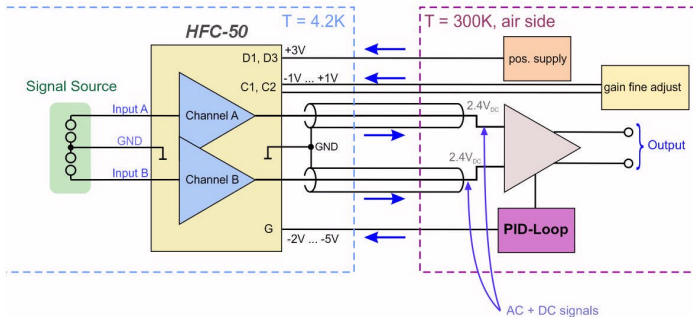


Figure: Commercial, cryogenic, low noise, high gain, dual pre-amp for transmission line signal extraction from cryogenic to room temperature environments.

26 Wien Filter

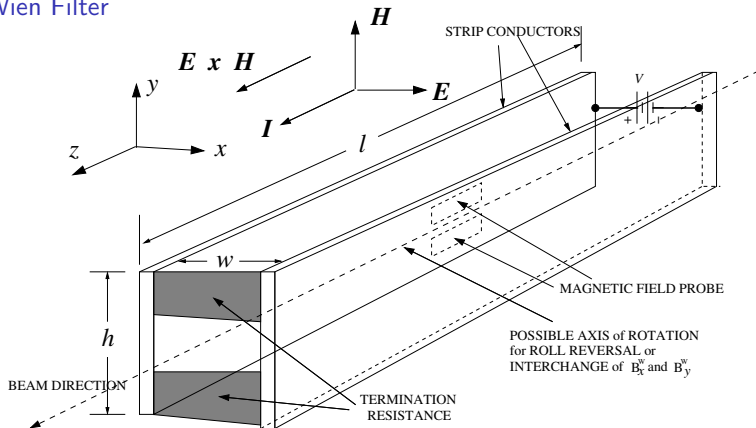


Figure: Stripline Wien filter dimensions. With electromagnetic power and beam traveling in the same direction, the electric and magnetic forces tend to cancel. Termination resistance R is adjusted for exact cancelation. For rolling polarization reversal, the Wien filter current to be reversed will be a conveniently low value, such as 5 A.

27 Wien reversal current bridge monitor

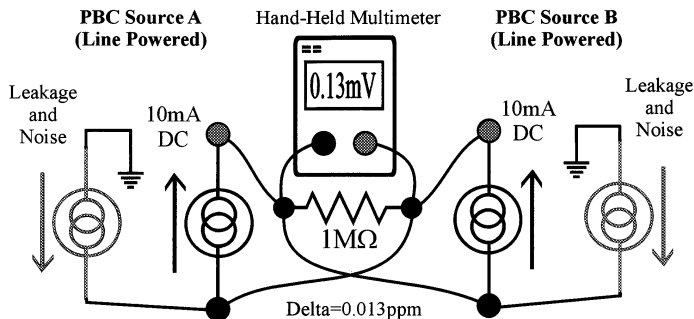


Figure: Current bridge used for high precision current monitoring. Copied from CERN, PBC reference. One current is the active current, the other a highly stable reference current. Even hand-held, 1 part in 10^8 precision is obtained. Wien current reversal precision will be monitored every run by recording the potentiometer voltage with Wien current in one arm and standard current in the other.

28 Achievable Precision (i.e. not including systematic error) say for electron

EDM in units of (nominal value) 10^{-29} e-cm = \tilde{d}

$2 \times \text{EDM}(\text{nominal})/\text{MDM}$ precession rate ratio:

$$2\eta^{(e)} = 0.92 \times 10^{-15} \approx 10^{-15}$$

duration of each one of a pair of runs = T_{run}

smallest detectable fraction of a cycle = $\eta_{\text{fringe}} = 0.001$

N_{FF} = EDM induced fractional fringe shift per pair of runs

$$= \frac{(2\eta^{(e)})\tilde{d}}{\eta_{\text{fringe}}} h_r f_0 T_{\text{run}} \quad \left(\text{e.g. } \tilde{d} \frac{10^{-15} \cdot 10 \cdot 10^7 \cdot 10^3}{10^{-3}} = 0.1\tilde{d} \right),$$

Assumed roll rate reversal error : $\pm \eta^{\text{rev.}} \stackrel{\text{e.g.}}{=} 10^{-10}$

$\sigma_{FF}^{\text{rev.}}$ = roll reversal error measured in fractional fringes

$$= \pm \frac{f^{\text{roll}} \eta^{\text{rev.}} T_{\text{run}}}{\eta_{\text{fringe}}} \quad \left(\text{e.g. } \pm \frac{10^2 \cdot 10^{-10} \cdot 10^3}{10^{-3}} = 10^{-2} \right).$$

particle	$ d_{\text{elec}} $ current upper limit e-cm	excess fractional cycles per pair of 1000 s runs	error after 10^4 pairs of runs e-cm	roll reversal error e-cm
neutron	3×10^{-26}			
proton	8×10^{-25}	$\pm 8 \times 10^3$	$\pm 10^{-30}$	$\pm 10^{-30}$
electron	10^{-28}	± 1	$\pm 10^{-30}$	$\pm 10^{-30}$

- ▶ Successful application of the method depends on two not yet established experimental methods: resonant polarimetry (promising theoretically) and “rolling polarization trap” operation—meaning stable, phase-locked, rolling polarization operation—(promising experimentally, at COSY).
- ▶ It is thermal noise in the resonant polarimeter that limits EDM measurement *precision*.
- ▶ A successful single beam fill will include at least one forward/backward reversal of the roll (not beam) direction, with roll frequency precisely measured both before and after.
- ▶ One (of many) successful single beam EDM measurements will consist of four data sets, roll forward and backward, with EDM effect on (spin wheel vertical) and off (spin wheel horizontal “background” measurement).

- ▶ Almost all AC magnetic fields have cancelled. Only pure DC (or rather less than 0.01 Hz) ΔB_r error field gives a spurious EDM signal.
- ▶ Only CW/CCW beam direction reversal (with vanishingly small vertical orbit displacement) can reduce this systematic error. But the beams do not need to be present at the same time.
- ▶ Alternate runs with beam direction reversed to “cancel” EDM systematic error due to residual radial magnetic field.
- ▶ By running on integer (non-zero) vertical tune Q_y (to magnify BPM sensitivity) local ΔB_r fields can be cancelled, using CW/CCW beams, with diametrically-opposite pairs of ΔB_r correctors.
- ▶ Expressed as EDM upper limit, measurement *precision* of 10^{-30} e-cm after year-long running, for either electrons and protons, can be expected.

- ▶ *Accuracy* at the same level as the *precision* will require average sign reversal accuracy of Wien filter length/strength product at the level of one part in 10^{11} , also averaged over one year.
- ▶ Apparatus constituting a single Wien filter will all be contained in a single, temperature regulated, limited vibration, magnetically shielded, highly isolated, etc. box.
- ▶ Emittance growth due to intrabeam scattering (IBS) has been seen as a serious impediment to EDM measurement. With ultra-low Q_y not required, running “below transition”, which tends to suppress beam growth due to IBS, will be possible.
- ▶ Spin coherence time SCT is greatly increased by Möbius ring operation.

33 Spin wheel stabilizing torques

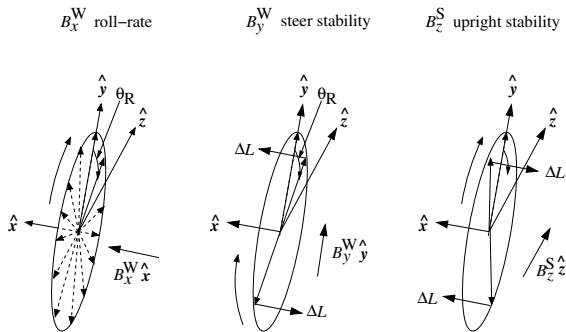


Figure: Roll-plane stabilizers: Wien filter $B_x^W \hat{x}$ adjusts the “wheel” roll rate, Wien filter $B_y^W \hat{y}$ steers the wheel left-right, Solenoid $B_z^S \hat{z}$ keeps the wheel upright.

- ▶ A Wien filter does not affect the particle orbit (because the crossed electric and magnetic forces cancel) but it acts on the particle magnetic moment (because there is a non-zero magnetic field in the particle's rest frame).

- ▶ A Wien torque

$$\hat{\mathbf{x}} \times (\hat{\mathbf{y}}, \hat{\mathbf{z}}) S = (\hat{\mathbf{z}}, -\hat{\mathbf{y}}) S$$

changes the roll-rate.

- ▶ A Wien torque

$$\hat{\mathbf{y}} \times (\hat{\mathbf{z}}, \hat{\mathbf{x}}) S = (\hat{\mathbf{x}}, -\hat{\mathbf{z}}) S$$

steers the wheel left-right.

- ▶ (Without affecting the orbit) a solenoid torque

$$\hat{\mathbf{z}} \times (\hat{\mathbf{x}}, \hat{\mathbf{y}}) S = (\hat{\mathbf{y}}, -\hat{\mathbf{x}}) S$$

can keep the wheel upright.

35 Resonant (Longitudinal) Polarimeter Response

- ▶ The Faraday's law E.M.F. induced in the resonator has one sign on input and the opposite sign on output.
- ▶ At high enough resonator frequency these inputs no longer cancel.
- ▶ The key parameters are particle speed v_p and (transmission line) wave speed v_r .
- ▶ The lowest frequency standing wave for a line of length l_r , open at both ends, has $\lambda_r = 2l_r$;

$$B_z(z, t) \approx B_0 \sin \frac{\pi z}{l_r} \sin \frac{\pi v_r t}{l_r}, \quad 0 < z < l_r. \quad (1)$$

- ▶ The (Stern-Gerlach) force on a dipole moment \mathbf{m} is given by

$$\mathbf{F} = \nabla(\mathbf{B} \cdot \mathbf{m}). \quad (2)$$

- ▶ The force on a magnetic dipole on the axis of the resonator is

$$F_z(z, t) = m_z \frac{\partial B_z}{\partial z} = \frac{\pi m_z B_0}{l_r} \cos \frac{\pi z}{l_r} \sin \frac{\pi v_r t}{l_r}. \quad (3)$$

- 36 At position $z = v_p t$ a magnetic dipole traveling at velocity v_p is subject to force

$$F_z(z) = \frac{\pi m_z B_0}{l_r} \cos \frac{\pi z}{l_r} \sin \frac{\pi(v_r/v_p)z}{l_r}. \quad (4)$$

Integrating over the resonator length, the work done on the particle, as it passes through the resonator, is

$$\Delta U(v_r/v_p) = m_z B_0 \left[\frac{\pi}{l_r} \int_{z=0}^{l_r} \cos \frac{\pi z}{l_r} \sin \frac{\pi(v_r/v_p)z}{l_r} dz \right]. \quad (5)$$

- See plot.

37 Energy lost in resonator

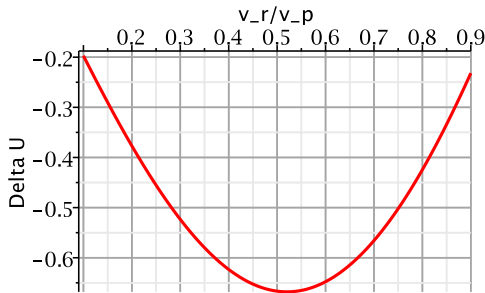


Figure: Plot of energy lost in resonator $\Delta U(v_r/v_p)$ as given by the bracketed expression in Eq. (5).

- ▶ For $v_r = 0.51 v_p$, the energy transfer from particle to resonator is maximized.
- ▶ **With particle speed twice wave speed, during half cycle of resonator, B_z reverses phase as particle proceeds from entry to exit.**